*Bulgarian Chemical Communications, Volume 47, Special Issue D (pp. 38 – 48) 2015*

# Multi-objective multivariable optimization of agglomerated cathode catalyst layer of a proton exchange membrane fuel cell

B. Kazeminasab[1*], S. Rowshanzamir[2,3], H. Ghadamian[4]

[1]*Department of Energy Engineering, Graduate College of Environment and Energy, Science and Research Branch, Islamic Azad University, Tehran, Iran. b.kazeminasab@srbiau.ac.ir*
[2]*School of Chemical Engineering, Iran University of Science and Technology. rowshanzamir@iust.ac.ir*
[3]*Fuel Cell Laboratory, Green Research Center, Iran University of Science and Technology.*
[4]*Department of Energy, Materials and Energy Research Center (MERC), Tehran, Iran. h.ghadamian@merc.ac.ir*
Received June 26, 2015, Revised September 10, 2015

Since the optimization objectives of the cathode catalyst layer (CCL) of a PEM fuel cell affect each other, thinking of them separately, would not be realistic and accurate; s o they must be solved simultaneously. In this study, a multi-objective multivariable optimization based on an agglomerate model, is performed and objective functions like current density and the cost of CCL are optimized under different variables. Decision variables include important or measurable parameters, namely platinum loading, ionomer volume fraction, agglomerate radius and porosity, and water saturation. Comparing these results with those of optimizations whose objectives are combined as a single-objective, found the optimization results have a good overlap at low current densities, however when increasing the current the results diverge. This deviation occurs as a result of interaction between objectives. The sensitivity analysis shows that the best range of platinum loading is 0.1 and 0.4 mg cm-2. The Pareto curve at the voltage of 0.6 V indicates that the best trade-off between the cost and the performance of the CCL is achieved, when the current density increases in the range of 5 % to 12 %, where the optimization objectives are met simultaneously.

**Keywords:** Agglomerate model, Cathode catalyst layer, Multi-objective optimization, Pareto curve, Trade-off.

## INTRODUCTION:

Cathode catalyst layer (CCL) is an important component in proton exchange membrane (PEM) fuel cells. In this layer, the proton current and oxygen molecules are electrochemically converted into an electron current [1]. The losses resulting from this conversion; include the limitation in the transportation of reactants and products, and poor oxygen reduction reaction (ORR) kinetics, which can reduce the efficiency of the fuel cells.

Modelling of the cathode catalyst layer is performed to attain a better discernment of the conditions, structure, transport properties and electrochemical reactions and also to evaluate the effect of variables on the performance. In general, there are three models to describe the CCL: (i) ultra-thin layer, (ii) pseudo-homogeneous and (iii) agglomerate models. Usually, the agglomerate model has the better representation of the catalyst layer (CL) compared to other models [2]. Thus, the overall accuracy of these models depends strongly on the description of the CL [3]. Therefore an agglomerate model has been considered in order to simulate the CCL.

Then, the optimization of CL is performed to improve the performance and reduce the expenses of the fuel cells. Since improving the performance and reducing the cost of CL simultaneously are crucial precondition for the commercialization of fuel cell, this research has been conducted to study multi-objective optimization (MOO) of the CCL. Many real problems require multi-objective evaluation [4] because their optimization objectives affect each other. Moreover, the inherent conflicting of the goals causes more difficulty during the calculation of the optimum solution. Hence, for the optimization study, a MOO coupled to above model is applied.

In the literature, several studies were presented for optimizing the PEM fuel cell or its CLs. Some of these studies are discussed below in brief and then the overall conclusions are also drawn at the end of this section. In order to obtain optimum distributions of catalyst loading and ionomer across the CCL of the PEM fuel cell, Song et al. [5] showed that the optimum distributions are linear when the optimization is performed using a single-variable, while the optimum distribution of ionomer remains linear, but that of catalyst loading becomes convex when the optimization is behaved as a two-variable problem. According to their results, the interaction of variables is significant and should not be ignored. Madhusudana and Rengaswamy [6] studied the

To whom all correspondence should be sent:
E-mail: b.kazeminasab@srbiau.ac.ir

optimization of the agglomerate CCL, in order to minimize the total amount of platinum and to maximize the current density, separately.

For the first time, Na and Gou [7] proposed a MOO technique with two objective functions of performance and expense to optimize fuel cell systems. They demonstrated a more cost-effective fuel cell system with a high- performance level will be obtained. Then Ang et al. [8] suggested a MOO technique for a general PEM fuel cell system, using the weighted-sum method. They showed that, a more efficient system was bigger, and vice versa. Overall, their results indicated that, to reach the most of the size-efficiency trade-off, the system must be operated at efficiency between 40 % and 47 %. Ang et al. [9] in another work, reviewed the methods and strategies of fuel cell system optimization, and then categorized the MOO into a bi-objective and a tri-objective optimal design. Secanell et al. [10] considered fuel cell Membrane-Electrode-Assembly for MOO. The objective was to simultaneously maximize the efficiency and minimize its production expenses. The results showed the expense - efficiency compromises, and they illustrated that considerable yields in the efficiency and cut in expenses were possible.

Srinivasarao et al. [11] individually considered some objective functions in order to optimize the CL. The optimized parameters of CL are vigorously influenced by the constraints and the objective functions. Khajeh-Hosseini et al. [12] improved a 1D agglomerate model for the CCL of a PEMFC to study the effects of catalyst layer variables on the activation loss. Additionally, the harmony search algorithm was utilized to get the optimal values of variables to minimize the activation overpotential of CL.

Tahmasbi et al. [13] applied a novel approximate to the MOO technique in the fuel cell system based on simultaneous power maximization and cost minimization by a genetic algorithm. Power maximization results at the peak power (1.95 kW), the unit expense of energy is $0.64. On the contrary, the expense minimization decreased the unit expense of energy to $0.33, while, output power was decreased to 0.93 kW. It means the optimization of fuel cell system is strangely influenced by the weighting factors of the objective functions. Mert and Özçelik [14] implemented MOO of a direct methanol fuel cell with three objective functions of power, energy and exergy efficiencies, and then calculated the optimal values of objective functions separately and simultaneously. According to these results, the best results drawn for the objectives, when considered separately, are larger than those when all the objectives are considered simultaneously. At last Feali and Fathipour [15] determined the trade-off curve between fuel utilization and output power density by genetic algorithm. They showed that to attain the optimum trade-off between the power and utilization, the current of the fuel cell should be less than 0.9 mW $cm^{-2}$.

Although recently a few multi-objective optimizations have been performed for the fuel cell system, the optimizations of CCL are restricted to single-objective ones, such as that of cost or performance. Since the objectives of optimization affect each other, considering the objective functions separately would not be realistic and accurate, so objective functions of CCL must be solved simultaneously. In all cases above, the interaction between the goals of the CCL was not taken into consideration, each goal was optimized separately. In this study, a multi-objective multivariate optimization (MOMO) based on an agglomerate model is performed for CCL of PEM fuel cell. This optimization utilized to study the cost and the performance trade-off concerned with the model of CCL. The fminimax and bvp4c functions of MATLAB software are aided in optimization and modelling stage, respectively. Objective functions are current density and cost of CCL, and decision variables include platinum loading, ionomer volume fraction, agglomerate radius and porosity, and water saturation.

This paper is organized as follows: Section 2 presents the CCL modelling. Section 3 describes the CCL optimization formulation based on this model. Section 4 provides the important results from the investigation of objectives and variables. Section 5 concludes the paper.

## CATHODE CATALYST LAYER MODELLING

Before any optimization can be done, the problem must first be modelled. The catalyst layer was modelled as an ultra-thin layer in the earlier models. Afterward, the catalyst layer is considered to be of finite thickness. Recently, microscopic images (SEM and TEM) have shown that the catalyst layer is built of Platinum/Carbon particles and a Nafion film, called agglomerates [16]. Agglomerate models have numerous parameters, including operational parameters, namely temperature, pressure and saturated liquid water, and structural parameters such as platinum loading, ionomer volume fraction, porosity and CL thickness, radius and porosity of agglomerate, etc.

Since the major variations occur in the diffusion direction of reactants (*Z* direction), a high-precision, one-dimensional model is applied to speed up the implementation of written code in the optimization stage. It's reasonable to assume an isothermal model in the low-temperature fuel cell where the generated heat is spent on the heating of the produced water.

In this study, a one-dimensional, isothermal, steady-state, agglomerate model is considered and developed for the CCL of a PEM fuel cell.

The agglomerate CL consists of Nafion ionomer, platinum and carbon particles as shown in Fig. 1. There are more details of agglomerate models in the references [3, 6, 12, 17].

Other assumptions of modelling are:

The void spaces between the agglomerates may be partially or fully filled with water

The PEMFC operates at steady-state and isothermal condition

The agglomerate particles are spherical in shape

Reaction kinetics are first-order with respect to the oxygen concentration

The gases are assumed to be ideal.

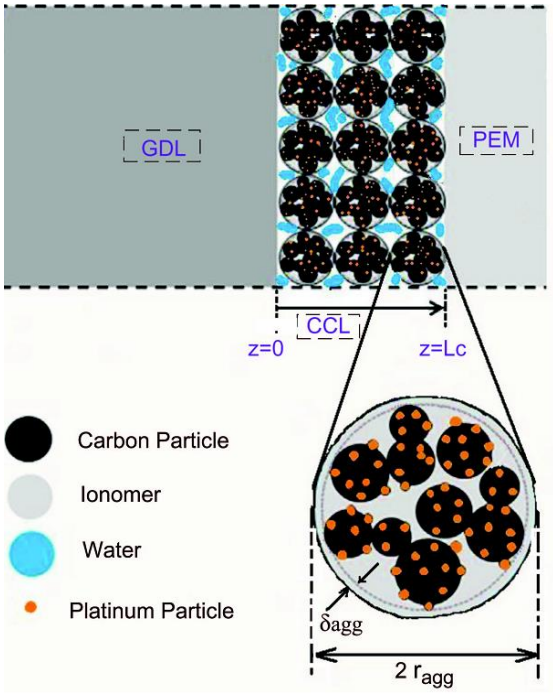


**Fig. 1.** Cathode catalyst layer based on agglomerate model.

## GOVERNING EQUATIONS

As the considered model is one-dimensional, isothermal and steady state, the CL phenomena consist of proton transfer, oxygen diffusion and overpotential losses along the vertical direction of catalyst layer (*Z* direction). Ohmic and concentration losses will be calculated when these parameters have been determined.

### *Current Profile*

The oxygen conservation within agglomerate in steady-state indicates:

$$\nabla . N_{O_2} = R_{O_2} \quad (1)$$

Where $R_{O_2}$ represents the oxygen consumption rate and $N_{O_2}$ shows flux of oxygen in the Nafion that is defined by Fick's diffusion law:

$$N_{O_2} = -D^{eff}_{O2,agg} \nabla C_{O_2} \quad (2)$$

Where $D^{eff}_{O2,agg}$ is the effective diffusion coefficient of oxygen inside agglomerate that is calculated by the Bruggeman's relation [6].

A combination of Eqs. (1) and (2) and expanding the produced equation leads to:

$$\frac{D^{eff}_{O_2,agg}}{r^2} \frac{d}{dr}\left(r^2 \frac{dC_{O_2}}{dr}\right) - k_1 . a . C_{O_2} = 0 \quad (3)$$

Equation (3) is a 2nd-order ODE which is solved analytically [17]:

$$C^* = \frac{\sinh(3\varphi r)}{r^* \sinh(3\varphi)}$$

$$\left(\text{Where: } \varphi = \frac{r_{agg}}{3}\sqrt{\frac{k_1 . a}{D^{eff}_{O_2,agg}}}\right), (4)$$

Now, we define $E_r$ as the agglomerate effectiveness factor as [17]:

$$E_r = \frac{\bar{R}_{O2}}{R_{O_2,max}} = \left[\frac{1}{\varphi}\left(\frac{1}{\tanh(3\varphi)} - \frac{1}{3\varphi}\right)\right], \quad (5)$$

The consumption rate of oxygen per unit volume of the catalyst layer can be linked to the current of protons i as:

$$R_{O_2}\frac{A}{a} = \frac{1}{4F}\nabla . i, \quad (6)$$

Where $\nabla . i$ can be substituted by di/dz for a one-dimensional study [10]:

$$\frac{di}{dz} = 4F\left(\frac{1}{E_r k_1 A} + \frac{\delta}{a_{agg} D_{O_2,N}}\frac{r_{agg+\delta}}{r_{agg}}\right)^{-1}\frac{C_{O_2}}{H_{O_2}}, \quad (7)$$

### *Oxygen Profile*

For the ORR, the consumption rate of oxygen is $(i_{tot}-i)/nF$. Hence the distribution of oxygen concentration in the CL is [6]:

$$\frac{dC_{O_2}}{dz} = \frac{i - I_\delta}{4FD^{eff}_{O_2,CL}}, \quad (8)$$

### *Overpotential Loss Profile*

The resistance against the migration of electron and proton in the catalyst layer is defined by Ohm's law [6]:

$$\frac{d\eta}{dz} = \frac{i}{k^{eff}} + \frac{i-I_\delta}{\sigma^{eff}}, \quad (9)$$

*Boundary Conditions*

According to Fig. 1 and ideal gas assumption, boundary conditions at *Z=0* are:

$$C_{O_2}\big|_{z=0} = \frac{P_{O_2}}{RT} = \frac{P_{O_2}}{1.33\exp(-\frac{666}{T})}\ ,\ i|_{z=0} = 0, \quad (10)$$

And boundary condition at $Z=L_C$ is:

$$i|_{z=L_c} = I_\delta \quad ,(11)$$

*Solution method*

Equations (7-9) along with boundary conditions Eqs. (10) and (11) form a coupled system of nonlinear ODEs with the unknown independent variables i, $C_{O_2}$ and η that control the transfer of protons, oxygen and electrons within the catalyst layer. In this study, the coupled system of equations is solved through coding in MATLAB software by shooting method, as shown in Fig. 2. After solving the system of equations and calculating the losses, the performance curve is drawn.

*Model validation*

This model was verified using a comparison with the experimental data conducted by Chang et al. [18] and also the non-isothermal, two-phase and three-dimensional model by Obut et al. [19] in Fig. 3. As seen over the whole range of the performance curve, a very good agreement between all results is obtained; therefore, if the agglomerate model including numerous operational and structural parameters were used, considering the assumptions such as the isothermal, one-dimensional and steady state could not reduce the accuracy of the results. The values of the input variables for the base case are shown in Table 1.

*Cathode catalyst layer optimization*

After the CL modelling has been conducted and its precision has been confirmed, CL optimization is performed. Modelling offers powerful tools and guidance for performance optimization.

To cut the costs of the fuel cells, the studies progress in two routes: replacing the platinum with suitable non-precious metal alternatives [20] and optimal design of the fuel cell to predict and understand phenomena occurring in the cell. Optimal designs of catalyst layers will be further classified according to their composition and structure [21].

The optimization problems sometime include more than one objective function needing to be optimized simultaneously. The process of optimizing a number of objective functions is called multi-objective optimization [4]. MOO is also known as multi-criteria [22] or multi-attribute optimization. In MOO it is not possible to find a single solution as an optimal solution for all of the functions together [4]. MOO consists of three phases: model building, optimization and decision making. After having found some solutions of the MOO problem, we must select a solution from this set [23]. One of the benefits of MOO is that it takes the interaction between the objectives into consideration.

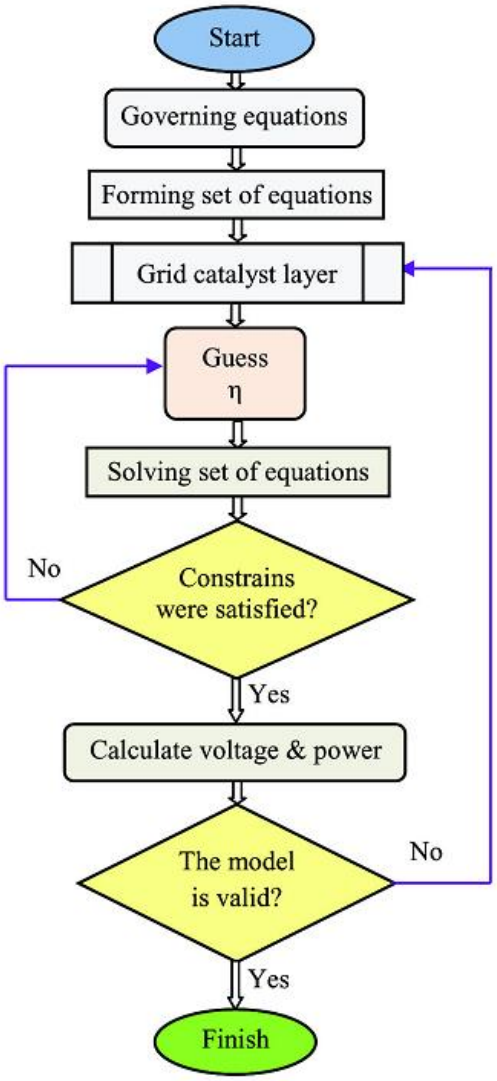


**Fig. 2.** Algorithm for solving the differential equations of CCL.

*Objective Functions*

Objective functions of CL optimization usually contain maximization of current density, output power, current density per Pt loading, and minimization of voltage losses, fuel cell size, and CL cost per power. This simulation can optimize many objective functions simultaneously but here, in order

to compare our results with existing results, two objective functions namely current density and CL's cost are used.

The CL is a combination of Pt/C and ionomer solution; therefore, the sum of platinum and ionomer costs is a good indicator of CL's cost. So in order to create the cost function of CL, the expression below is procured from curve fitting of $r_{Pt}$ and related cost data and the cost of Nafion solution [11]. The manufacture cost of CL depends on the synthesis technology and the laboratory, and could be added to the cost function of the catalyst layer only if it was determined.

The objective function of current density is also obtained from solving the modelling equations. A minus is added by the current density function, so that the two objective functions could be minimized.

**Table 1.** Input data used for base case in modelling stage [10, 17-19].

| Parameters | Quantity | Value / Units |
|---|---|---|
| T | Temperature | 60 °C |
| P | Pressure | 1.1 bar |
| $X_{O2}$ | Oxygen mole fraction in CCL | 21 % |
| s | Liquid water saturation | 0.5 |
| $L_C$ | Catalyst layer thickness | 30 μm |
| $R_{ohmic}$ | Ohmic resistance | $0.47\times10^{-4}$ Ωm$^2$ |
| $m_{Pt}$ | Pt mass loading | 0.003 kg m$^{-2}$ |
| $\rho_{Pt}$ | Density of Pt | 21,400 kg m$^{-3}$ |
| $\rho_C$ | Density of Carbon | 1800 kg m$^{-3}$ |
| $r_{Pt/c}$ | Platinum mass ratio on Pt/C particles | 0.2 |
| $C_{O2, ref}$ | Reference $O_2$ concentration | 2.28 mol m$^{-3}$ |
| $\alpha_C$ | Transfer factor of Cathode | 1.0 |
| $\alpha_a$ | Transfer factor of Anode | 0.5 |
| κ | Protonic conductivity | 300 Ω$^{-1}$m$^{-1}$ |
| σ | Electronic conductivity | 72,000 Ω$^{-1}$ m$^{-1}$ |
| τ | CL tortuosity | 1.5 |
| $r_{agg}$ | Radius of agglomerate | 0.3 μm |
| $\varepsilon_{agg}$ | Spherical agglomerate porosity | 0.45 |
| $\delta_{agg}$ | Thickness of agglomerate | 30 nm |
| $\varepsilon_{CL}$ | CL porosity | 0.2 |
| $\varepsilon_g$ | GDL porosity | 0.74 |
| $L_{mc}$ | Volume fraction of membrane in the CL | 0.3 |
| $L_{gc}$ | Volume fraction of GDL in the CL | 0.1 |
| Ap | Adjustable parameter | If i < 2000 Ap=3 else Ap=0.3 |

**Table 2.** Comparing the results of multi-objective optimization and optimization of Ref. [11].

| Results of Ref. [11]: | | | | | | |
|---|---|---|---|---|---|---|
| Voltage (V) | Current density / mA cm$^{-2}$ | | Cost function / $ W$^{-1}$ | | % Gain in performance | % Gain in cost |
| | Base case | Optimized case | Base case | Optimized case | | |
| 0.8 | 265.47 | 292.02 | 0.61182 | 0.5212 | 10 | 14.81 |
| 0.6 | 1081.7 | 1189.9 | 0.2002 | 0.1339 | 10 | 33.12 |
| 0.4 | 1895.3 | 2084.8 | 0.17139 | 0.1021 | 10 | 40.43 |
| Results of this work: | | | | | | |
| 0.8 | 265 | 290 | 0.613 | 0.523 | 10 | 14.68 |
| 0.6 | 1070 | 1180 | 0.201 | 0.152 | 10 | 24.38 |
| 0.4 | 1880 | 1980 | 0.173 | 0.128 | 5 | 26.01 |

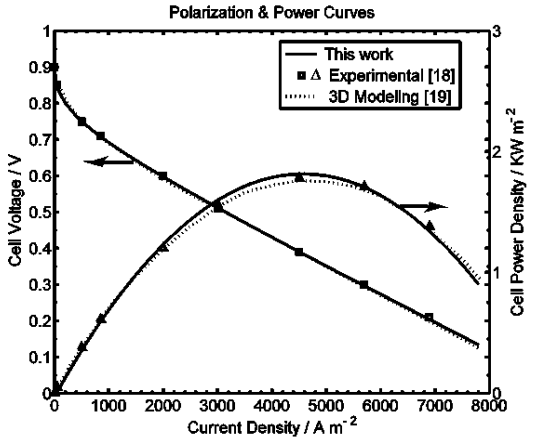


**Fig. 3.** Comparing the modelling results with results in [18, 19].

Finally, the following relations are used for the cost function of carbon-supported platinum and the cost function of ionomer, respectively:

$$C_1=251.7\ r_{pt/C}+6.6092\ ,\ C_2=24.0566 \quad /\$\ g^{-1}, \quad (12)$$

Weight of carbon-supported platinum and weight of ionomer come from the following relations, respectively:

$$\begin{cases} W_{Pt}+W_C=m_{Pt}\times 10^{-3}\ \text{Area}/r_{Pt/C} \quad /\ \text{g}, \\ W_i= m_{Pt}\times 10^{-3}\text{Area}/r_{Pt/C}\times f_i/(1\text{-}f_i) \quad /\ \text{g} \end{cases} \quad (13)$$

Where fi (mass ionomer ratio) will be obtained from the following relation:

$$f_i= \frac{L_{mc}\ \rho_i\ r_{Pt/C}\ L_C\times 10^5}{m_{Pt}+L_{mc}\ \rho_i\ r_{Pt/C}\ L_C\times 10^5}, \quad (14)$$

Finally, the objective functions are obtained from the following relations:

$$f_1=-I_\delta \quad /\text{A cm}^{-2}, \quad (15)$$

$$f_2=(\ C_1\ (W_{Pt}+W_C\ )+C_2W_i) \quad /\$, \quad (16)$$

*Variables and constraints*

There are many variables in the catalyst layer structure that influence the efficiency of the fuel cells. These variables are a combination of structural and operational parameters. Operational parameters include temperature, pressure and water saturation, and structural variables include thickness of Nafion film, agglomerate radius and porosity, catalyst loading, carbon loading, carbon-platinum ratio, Nafion fraction, GDL passing into CL, GDL porosity, CL porosity and thickness.

Although this study is theoretical, the decision variables can be controlled during the manufacture of the PEM fuel cell as follows: Agglomerate radius and porosity, and water saturation can be controlled through the synthetic techniques of MEA, pore formers, and water management, respectively. The catalyst layer thickness and ionomer fraction depend on the amount of used ionomer, carbon and platinum.

In a written program, we can investigate all variables simultaneously, but here only important or measurable parameters are scrutinized. These parameters include: platinum loading, ionomer volume fraction, agglomerate porosity, agglomerate radius and water saturation.

To avoid unrealistic design criteria, the upper and lower limits below are applied to the parameters:

$$\begin{cases} x= [m_{pt},\ l_{mc},\ \varepsilon_{agg},\ r_{agg},\ s] \\ lb=[0.01,\ 0.1,\ 0.1,\ .01,\ .01]; \\ ub=[2.0,\ 0.9,\ 0.9,\ 0\ .5,\ 0.7]; \end{cases} \quad (17)$$

Constraints of the multi-objective optimization problem can be imposed on problem variables or objective functions. Constraints of variables are defined as volume fraction of solid, ionomer and void in the CL:

$$L_{mc}\begin{cases} \varepsilon_v=\varepsilon_{CL}=1-\frac{m_{Pt}}{L_C}\left(\frac{1}{\rho_{Pt}}+\frac{1-r_{Pt/C}}{r_{Pt/C}\cdot\rho_c}\right)- \\ 0<\varepsilon_v<1 \\ \varepsilon_i=L_{mc}=\frac{f_i}{1-f_i}\frac{1}{\rho_i}\frac{m_{Pt}}{r_{Pt/C}L_C} \quad 0<\varepsilon_i<1, \end{cases}$$

$$\varepsilon_s=1-\varepsilon_v-\varepsilon_i=\frac{m_{Pt}}{L_C}\left(\frac{1}{\rho_{Pt}}+\frac{1-r_{Pt/C}}{r_{Pt/C}\cdot\rho_c}\right) \quad 0<\varepsilon_s<1 \quad (18)$$

In addition, constraints imposed on objective functions, such as the cost and the performance, could be seen as CL cost less than a specific value (e.g., base cost) or its performance greater than the base value, e.g., up to 20 %.

$$\begin{cases} \text{CL cost}_{\text{Optimized}} < \text{CL cost}_{\text{Base case}} \\ \text{Curren density}_{\text{Optimized}} - \text{Curren density}_{\text{Base case}} > (0-20)\ \% \end{cases} \quad (19)$$

*Solution algorithm*

However the possible solutions to the MOO are usually in conflict with several objectives, but the Pareto set has minimum conflict [24]. One of the methods most used to solve a MOO in order to obtain a Pareto-optimal set is the min-max method. This method tries to find a feasible design that minimizes its distance from the ideal design [25]. This method also uses the nonlinear programming algorithm, a sequential quadratic programming (SQP). There are two functions to solve constrained nonlinear MOO in MATLAB: fminimax and fgoalattain, both of which use a SQP method [26, 27].

In this study, we use the fminimax method because the fgoalattain method is more complicated

due to use the weighting coefficients. However, both methods have local solutions [5]. Due to the low range of variables and because a local minimum for a convex function is always a global minimum, this disadvantage does not cause difficulties. On the other hand, same results are obtained for different initial guesses.

In this research, the current density and the cost of CL are optimized under various conditions through the MOO technique using the min-max method. First of all, coding with MATLAB software, the set of equations obtained from the modelling stage is calculated using the bvp4c function as shown in the algorithm in Fig. 2. Then, MOO functions are solved through fminimax function and via Eq. (20). The fminimax is formed of objective functions, variables and constraints according to Eq. (20). The optimization algorithm is shown in Fig. 4.

$$\begin{cases} \text{fminimax} & f_1, f_2 \\ \text{w.r.t.:} & m_{pt}, l_{mc}, \varepsilon_{agg}, r_{agg}, s \end{cases} \quad (20)$$

Subject to: $0 \le \varepsilon_v \le 1$ , $0 \le \varepsilon_i \le 1$ and $0 \le \varepsilon_s \le 1$

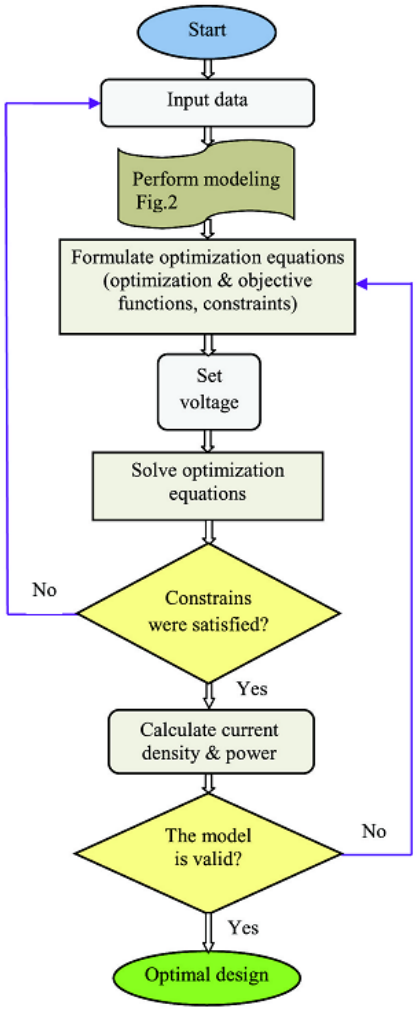


**Fig. 4.** Algorithm for performed multi-objective optimization.

*Optimization validation*

This simulation can optimize many objective functions simultaneously, but here, in order to compare our results with the available result, only two objective functions, namely maximization of current density and minimization of CL cost, are used. Our results are arranged in such a way that they can be compared with results in Ref. [11]. Input data are also the same as those of Ref. [11], with the rest of the data used in Table 1. Many variables are also considered in the catalyst layer modelling, but here only important or measurable parameters are scrutinized. These parameters include: platinum loading, carbon-platinum ratio, ionomer volume fraction, agglomerate porosity and radius, and water saturation.

Optimization results at three voltages, including high, medium and low voltages, and two states, base case and optimized case, are compared in Table 2 and Fig. 5. As can be seen, the results of both models at the base case conformed at high, medium and low voltages; therefore, their results can be compared. Optimization results show a good agreement at low current density. Increasing current density, which causes an increase in losses and cost-saving resulting from using less platinum, makes a divergence appear between optimizations. It occurs because in the above-mentioned reference, two objectives are actually optimized through a single objective manner, while in our study two objectives are used separately and simultaneously, so interactive effects of objectives are considered.

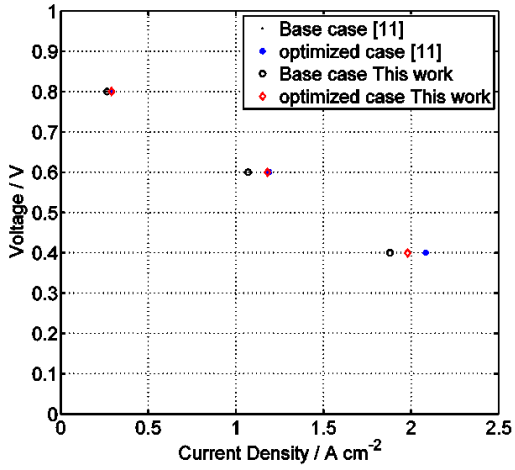


**Fig. 5**. Comparing these results and results in [11] at base case and optimized case.

## RESULTS AND DISCUSSION

Since the amount of catalyst is the most important factor influencing the optimization objectives of the catalyst layer (performance and cost), before any

optimization is done, the effect of platinum on the performance is investigated in various voltages.

Pt loading diagram is drawn *vs.* current density and cost at the voltages of 0.8, 0.6 and 0.4 V in Fig. 6. The slope of the curve is very small where the platinum loading is larger than 0.4 mg $cm^{-2}$; that is, increasing a large amount of platinum leads to small changes in current density, so it would not be economical to increase the platinum loading any more than that. By contrast, the slope of the curve is very sharp where the platinum loading is less than 0.1 mg $cm^{-2}$; it means that, in order to reduce the cost, a large drop in the current density occurs through reducing Pt in small scales; therefore, the reduction of Pt in larger scales would not be technically justified. So, the best compromise between the cost and the performance should be achieved within this platinum range.

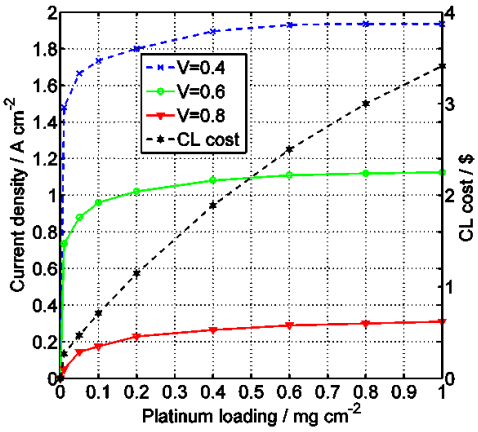


**Fig. 6.** Diagram of platinum loading *vs.* current density at the voltages of 0.8, 0.6 and 0.4 volt.

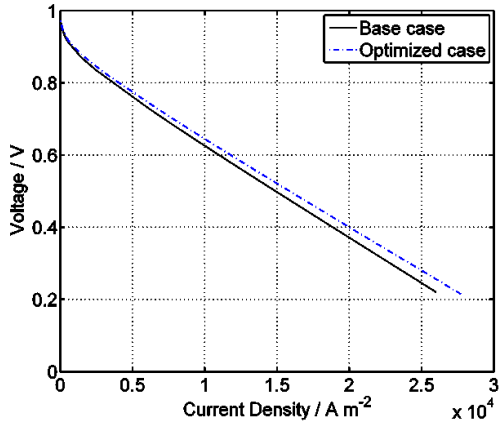


**Fig. 7.** Performance curve of fuel cell for both the base case and the multi-objective optimization case.

The catalyst layer cost increases 166 % at all three voltages in the above platinum ranges while the current density increases by 51.4 % at the voltage of 0.8 V, 12.7 % at the voltage of 0.6 V and 9.2 % at the voltage of 0.4 V; thus, the current is more dependent on the amount of platinum at high voltages, due to the importance of activation overpotential, instead, it is far less dependent at low voltages.

Figure 7 demonstrates the performance curve of the fuel cell in both cases; base case and multi-objective optimization case. In Fig. 7, one of the objectives, namely cost, is considered the same as base cost, and another objective, namely performance, is optimized. Although the amount of increase in the CL performance is higher at the high currents, its relative increase is higher at the low current densities.

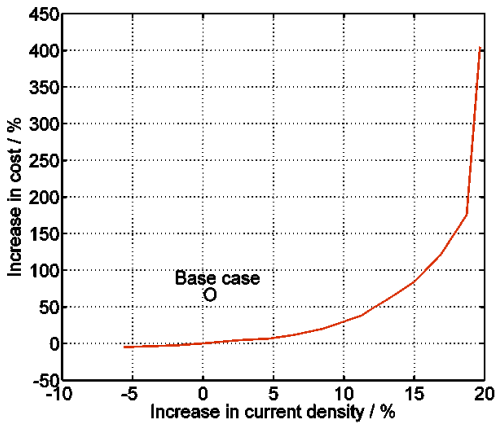


**Fig. 8.** Pareto curve for multi-objective optimization of catalyst layer at the voltage of 0.6 V.

In Fig. 8, a Pareto curve is drawn to optimize the objectives of performance and cost of the CL at the voltage of 0.6 V, where the base case (voltage 0.6 V, current 1.07 A $cm^{-2}$ and cost 1.819 $) is also marked with a circle. With multi-objective optimization at the base case current density, first the cost suddenly dropped compared to the base case, and then to increase the current density, the cost gradually increases. As shown in the graph on the left, the slope of the curve is very smooth, which shows that increasing the current density does not lead to too high a price; therefore, the current density can be increased as necessary. In the graph on the right, a slight rise in current leads to an increase in the cost several times, so increasing the performance in this area would not be economical; therefore, the trade-off between the cost and the performance is achieved, depending on the kind of application, when the current density increases in the range of 5 % to 12 %. In this range, the optimization objectives are met simultaneously; that is, the current is more than the base and the cost is lower than the base case.

In Fig. 9, a Pareto curve is drawn as the cost-power ratio *vs.* current at the voltage of 0.6 V. The above base case is also marked with a circle to compare. Here, a compromise is achieved between the objectives of cost-power ratio and current density

in the current density range of 1.13-1.23 A $cm^{-2}$ depending on the decision maker. Likewise, the current is more than the base and the cost is lower than the base case simultaneously.

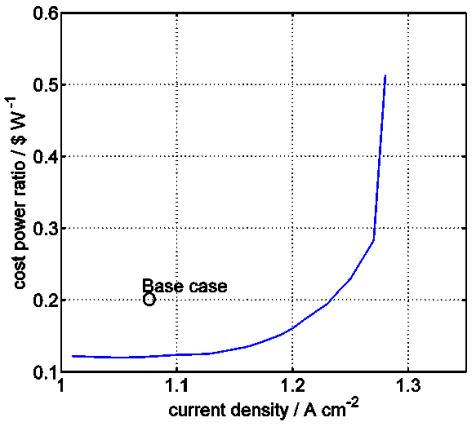


**Fig. 9.** Pareto curve for multi-objective optimization of catalyst layer at the voltage of 0.6 V: as term of cost power ratio *vs.* current density.

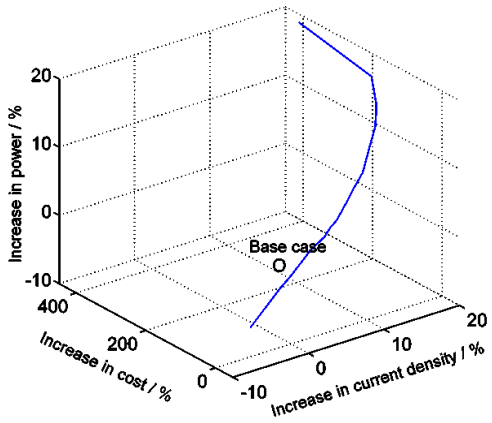


**Fig. 10.** Pareto curve as term of current density, cost, and power at the voltage of 0.6 V.

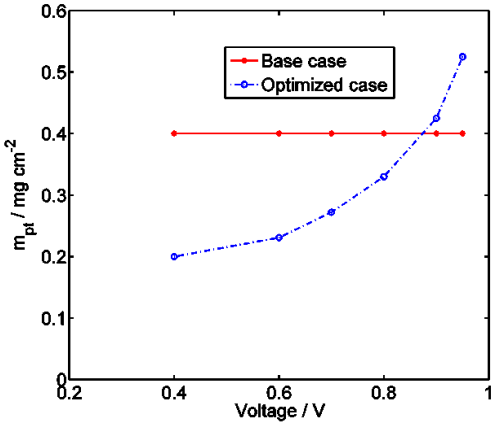


**Fig. 11.** Comparing the amount of platinum loading in both the base case and optimized case.

A Pareto curve for the three objective functions of current density, cost and power is drawn at the voltage of 0.6 V in Fig. 10. The diagram is drawn three-dimensionally in order to compare those variations caused by price, although the two functions of current density and power are not independent. As shown, the slopes of the current and the power are smooth, but the slope of the cost will be steep, particularly at the high currents; so even if the cost increases so much at higher currents, the current in these conditions cannot increase more than 20 %.

In Fig. 11, the platinum loading is compared in the base case and optimized case. As can be seen, a large amount of platinum is necessary due to the importance of activation overpotential caused by beginning the reaction at the high voltages. Even the Pt loading in the optimized case is higher than the base case. Conversely, less platinum is required at low voltages or high current densities because of the stronger effect of ohmic and mass transport losses. So, less platinum is consumed and costs are saved more significantly.

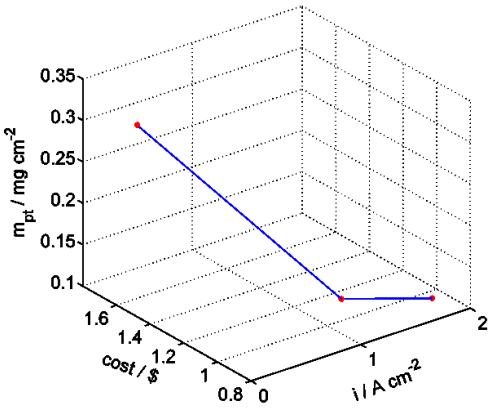


**Fig. 12**. Objective functions *vs.* platinum loading ($m_{Pt}$).

In this section, objective functions of current density and cost are plotted *vs.* two optimized decision variables at the voltages of 0.8, 0.6 and 0.4 volts. In Figs. 12, 13, current density is considered the same as base case and cost is optimized.

In Fig. 12, objective functions are plotted *vs.* platinum loading ($m_{Pt}$). Platinum loading has a direct and strong effect on CL cost, so usage of it must be reduced as far as possible. As shown, at low current densities, large amounts of platinum are necessary due to the activation overpotential caused by beginning the reaction that leads to increase in cost. Conversely, for the same reasons as in Fig. 11, less platinum is required at high current densities, so the cost decreases.

In Fig. 13, objective functions are plotted *vs.* ionomer volume fraction (lmc). Ionomer content also directly effects CL cost, so usage of it must be reduced as far as possible. Ionomer volume fraction has two opposing effects on CL performance. Large

amounts of lmc lead to reduced catalyst layer porosity, and as a result a decrease in the oxygen diffusion coefficient. On the other hand, according to Bruggeman's correction, the effective protonic conductivity increases, and hence CL performance increases. In high current densities, the effect of effective protonic conductivity dominates more clearly the effect of oxygen diffusion. Therefore, as shown, although more ionomer is used at high current densities, total cost is decreased.

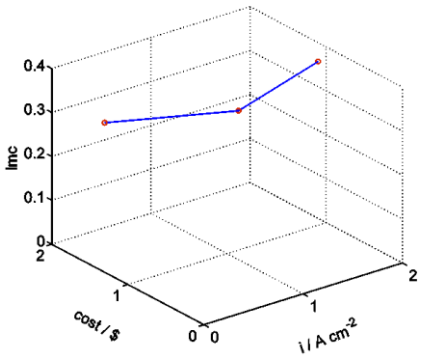


**Fig. 13.** Objective functions *vs.* ionomer volume fraction (lmc)

## CONCLUSIONS

After the CL modelling has been conducted and its precision has been confirmed, catalyst layer optimization is performed. In this study, objective functions such as power, current density and CL cost are optimized under various conditions using the multi-objective optimization technique through the min-max method.

The results of this study were compared with those of Ref. [11] to validate the performed optimization. This comparison suggested that the results of optimizations are in good agreement at low currents, however when increasing the current the results diverge, caused by increasing the amount and the number of losses. In fact, this deviation is due to the number of objectives; that is, whether single-objective or multi-objective optimization is employed.

The Pt loading curve is drawn *vs.* current density and cost at the voltages of 0.8, 0.6 and 0.4 V. It determines that increasing a large platinum loading leads to small changes in current density where the platinum loading is larger than 0.4 mg $cm^{-2}$. Conversely, a large drop in the current density occurs through reducing Pt at small scales, where the platinum loading is less than 0.1 mg $cm^{-2}$. So the best compromise between the efficiency and the cost should be attained within this platinum range.

The performance curve demonstrates that in both cases, base case and multi-objective optimization case, although the increase in the CL performance is higher at high currents, its relative increase is higher at low currents.

The Pareto curve demonstrates that to optimize the objectives of performance and cost of the CL at the voltage of 0.6 V, the trade-off between the cost and the performance is achieved, depending on the kind of application, when the current density increases in the range of 5 % to 12 %. In this range, the optimization objectives are met simultaneously; that is, the current is more than the base form and the cost is lower than the base form.

The platinum loading is compared in the base form and optimized form, where the large amount of platinum is necessary due to the importance of activation overpotential caused by beginning the reaction at high voltages. Even the Pt loading in the optimized case is higher than the base case. Conversely, less platinum is required at low voltages or high current densities. So, lower platinum is consumed and costs are saved more significantly.

*Nomenclature*

| | |
|---|---|
| a | active surface area within the agglomerate / $m^{-1}$ |
| $a_{agg}$ | total external area of active sites of agglomerate per unit volume of CL / $m^{-1}$ |
| A | total active area of agglomerate per unit volume |
| c | of CL / $m^{-1}$ |
| CL | concentration / mol $m^{-3}$ |
| $D_{O2}$ | Catalyst Layer |
| $D_{Kn}$ | diffusion coefficient / $m^2$ $s^{-1}$ |
| Er | Knudsen diffusion coefficient / $m^2$ $s^{-1}$ |
| fi | effectiveness factor |
| F | mass ionomer ratio |
| GDL | Faraday constant 96,485 /coulombs $mol^{-1}$ |
| $H_{O2}$ | Gas Diffusion Layer |
| i | dimensionless Henry's constant |
| $I_\delta$ | local current density /A $m^{-2}$ |
| $k_l$ | cell current density /A $m^{-2}$ |
| $L_C$ | reaction rate constant / m $s^{-1}$ |
| $L_{g,c}$ | catalyst layer thickness / m |
| $L_{m,c}$ | volume fraction of GDL penetrating into the CL |
| $m_{Pt}$ | volume fraction of ionomer phase in the CL |
| $m_C$ | platinum mass loading / kg $m^{-2}$ |
| $N_{O2}$ | carbon mass loading / kg $m^{-2}$ |
| ODE | molar flux of dissolved oxygen in the ionomer phase of an agglomerate |
| P | Ordinary Differential Equation |
| $r_{agg}$ | Pressure / Pa |
| $r_{Pt}$ | agglomerate radius / m |
| R | mass fraction of platinum to Pt/C articles |
| $\overline{R}$ | dissolved oxygen rate per unit of agglomerate |
| s | /mol $m^{-3}$ $s^{-1}$ |
| T | universal gas constant 8.314 /J $mol^{-1}$ $K^{-1}$ |
| W | liquid water saturation |
| r, z | temperature / K |
| $\delta_{agg}$ | weight |
| $\varepsilon_{agg}$ | coordinate / m |
| $\varepsilon_{CL}$ | ionomer film thickness,m |
| $\varepsilon_g$ | spherical agglomerate porosity |
| $\varepsilon_i$ | CL porosity |
| $\varepsilon_s$ | GDL porosity |
| $\varepsilon_v$ | volume fraction of ionomer |
| $\eta$ | volume fraction of solids |

| | |
|---|---|
| $\rho_c$ | volume fraction of voides |
| $\rho_{Pt}$ | activation overpotential / V |
| $\sigma$ | carbon density / kg $m^{-3}$ |
| $\kappa$ | platinum density / kg $m^{-3}$ |
| $\varphi$ | electronic conductivity / $Sm^{-1}$ |
| $\tau$ | protonic conductivity / $Sm^{-1}$ |
| | Thiele module |
| a | CL tortuosity |
| c | Subscription**s** |
| agg | anode |
| $O_2$ | cathode |
| N | agglomerate |
| r | oxygen |
| 1 | Nafion |
| CL | radius |
| C | first-order reaction |
| ref. | catalyst layer |
| tot. | catalyst layer boundary |
| | reference condition |
| eff | total |
| * | Superscriptions |
| | effective |
| | concentration or radius ratio |

REFERENCES:


1. A.A. Kulikovsky, *Electrochim. Acta*, **130,** 826 (2014).
2. L. Xing, X. Song, K. Scott, V. Pickert, W. Cao, *Int. J. Hydrogen Energy*, **38**, 14295 (2013**)**.
3. F.C. Cetinbas, SG. Advani, AK. Prasadz, *J. Electrochem. Soc.* **161**, F803 (2014**)**.
4. E. Goodarzi, M. Ziaei, E. Zia Hosseinipour, Introduction to Optimization Analysis in Hydrosystem Engineering, Springer, Switzerland, 2014.
5. D. Song, Q. Wang, Z. Liu, M. Eikerling, Z. Xie, T. Navessin, S. Holdcroft, *Electrochim. Acta,* **50**, 3347 (2005).
6. R. Madhusudana Rao, R. Rengaswamy, *Chem. Eng. Res. Des.* **84**, 952(2007**)**.
7. W. Na, B. Gou, *J. Power Sources* **166**, 411 (2007).
8. S.M.C. Ang, DJL. Brett, S. Fraga, *J. Power Sources,* **195**, 2754 (2010).
9. SMC. Ang, S. Fraga, NP. Brandon, NJ. Samsatli, D. Brett, *Int. J. Hydrogen Energy* **36**, 14678 (2011**)**.
10. M. Secanell, R. Songprakorp, A. Suleman, N. Djilali, *Energy Environ. Sci*., **1**, 378 (2008**)**.
11. M. Srinivasarao, D. Bhattacharyya, R. Rengaswamy, S. Narasimhan, *Chem. Eng. Res. Des.*, **89**, 10 (2011**)**.
12. N. Khajeh-Hosseini-Dalasm, M. Fesanghary, K. Fushinobu, K. Okazaki, *Electrochim. Acta,* **60**, 55 (2012**)**.
13. A.A. Tahmasbi, A. Hoseini, R. Roshandel, *Int J Sustain Energ* **, 34**, 283 (2015**)**.
14. SO. Mert, Z. Özçelik, *Int. J. Energy Res.*, **37**, 1256 (2013).
15. M.S. Feali, M. Fathipour, *Russ. J. Electrochem.*, **50**, 561 (2014).
16. D. Castagne, Mathematical modeling of PEM Fuel Cell cathodes," MS Thesis, Department of Chemical Engineering, Queen's University, Kingston, Ontario, Canada, 2008.
17. M. Moein-Jahromi, MJ. Kermani, *Int. J. Hydrogen Energy,* **37**, 17954 (2012**)**.
18. W.R. Chang, JJ. Hwang, FB. Weng, SH. Chan, *J. Power Sources* , **166**, 149 (2007).
19. S. Obut, E. Alper, *J. Power Sources* **196**, 1920 (2011).
20. R. Othman, AL. Dicks, Z. Zhu, *Int. J. Hydrogen Energy* **37**, 357 (2012).
21. D.P. Wilkinson, J. Zhang, R. Hui, J. Fergus, X. Li, Proton Exchange Membrane Fuel Cells: Materials Properties and Performance. Taylor and Francis Group, USA, 2010.
22. G.P. Rangaiah, A. Bonilla-Petriciolet. Multi-objective optimization in chemical engineering: developments and applications, John Wiley & Sons, 2013.
23. Y. Collette, P. Siarry. Multiobjective Optimization Principles and Case Studies. Springer, New York, 2004.
24. S.O. Mert, Z. Özçelik, Y. Özçelik, I. Dinçer, *Appl. Therm. Eng.* , **31**, 2171 (2011).
25. O.B. Augusto, F. Bennis, S. Caro, *Pesquisa Operacional* ,**32**, 331 (2012).
26. E.B. Magrab, Sh. Azarm, B. Balachanran, JH. Duncan, KE. Herold, GC. Walsh, An Engineer's Guide to MATLAB with Applications from Mechanical, Aerospace, Electrical, Civil, and Biological Systems Engineering. Third Edition, Prentice Hall, USA, 2011.
27. Optimization Toolbox of Matlab: User's Guide (2011b). MathWorks Incorporated; 2011.